Supplementary Information

High-Performance $LiFePO_4$ Regeneration through Na-Induced Lattice Activation and Conductivity Rewiring

Jiale Zhang[1], Shaofeng Li[2, 3], Yan Yan[4], Jiexiang Li[1], Zeyu Dong[1], Peng Ge[1], Yue Yang[1, 5, 6]*, Jie Zeng[2, 4]*

[1]School of Minerals Processing and Bioengineering, Central South University, Changsha 410083, China

[2]Hefei National Research Center for Physical Sciences at the Microscale, Chinese Academy of Sciences Key Laboratory of Strongly-Coupled Quantum Matter Physics, Key Laboratory of Surface and Interface Chemistry and Energy Catalysis of Anhui Higher Education Institutes, Department of Chemical Physics, University of Science and Technology of China, Hefei, Anhui 230026, China

[3]State Key Laboratory of Precision and Intelligent Chemistry, School of Chemistry and Materials Science, University of Science and Technology of China, Hefei, Anhui 230026, China

[4]School of Chemistry & Chemical Engineering, Anhui University of Technology, Ma'anshan, Anhui 243002, People's Republic of China

[5]State Key Laboratory of Mineral Processing, Beijing 410083, China

[6]Engineering Research Center of Ministry of Education for Carbon Emission Reduction in Metal Resource Exploitation and Utilization, Central South University, Changsha 410083, China

*e-mail: Yue Yang (yangyue18@csu.edu.cn), Jie Zeng (zengj@ustc.edu.cn)

Chemicals and materials

All chemical agents, such as C_2H_5OH and sucrose, were procured from Macklin Company. These chemical reagents were directly applied to recycle discarded LFP cathodes without additional purification steps. The discarded LFP cathode sheets were sourced from a company located in Hunan, China. Meanwhile, LFP cathodes, along with coin cell battery components, were obtained from Guangdong Couldrd New Energy Technology Co., Ltd. The components included coin cells, Celgard 2500 separator, polyvinylidene fluoride (PVDF), carbon black, aluminum (Al) foil, and metal discs. The electrolyte, a mixture of 1 M $LiPF_6$ dissolved in a volumetric ratio of 1:1:1 ethylene carbonate (EC), diethyl carbonate (DEC), and dimethyl carbonate (DMC), was purchased from DoDochem.

Procedure for the regenerated LFP

Harvesting $LiFePO_4$ material

Spent LFP batteries were first discharged in a saturated sodium chloride (NaCl) solution; this process continued until their voltage fell to below 1.0 V. After discharge, the batteries were manually disassembled to separate and collect the separator, as well as the cathode and anode sheets. To prepare spent LFP cathode materials, the pre-cut cathode sheets were soaked in deionized water, which allowed for the detachment of the aluminum (Al) foil from the cathode material. The cathode samples obtained from this step were then placed in an oven and dried at 70 ^oC for 3 hours to eliminate any residual moisture. Lastly, the dried cathode materials were ground for 5 minutes using a grinding device, resulting in the formation of powdered LFP samples. These powdered samples were designated as spent LFP, abbreviated as SLFP.

Spent LFP regeneration

Initially, the spent LFP was disassembled to obtain spent flakes. Subsequently, Li_2CO_3 and Na_2CO_3 were prepared at mass ratios of 100:0, 97.5:2.5, 95:5, and 90:10. An amount of Li_2CO_3 or Li_2CO_3/Na_2CO_3 1.1 times that corresponding to the lithium deficiency was required. The spent LFP, Li_2CO_3 and Na_2CO_3 were mixed in anhydrous ethanol using a ball-milled for 2 hours. Then, a sand bath at 80 ℃ was employed to evaporate the ethanol. The resulting product was heated in air at 500 ℃ to eliminate the conductive agent and binder. Next, 2 g of the oxidized material and 0.3 g of sucrose were ball-milled in 20 ml of anhydrous ethanol at a speed of 400

rpm for 2 hours. The obtained mixture was dried at 50 ℃ for 3 hours to remove the ethanol. After that, the dried material was preheated at 350 °C for 4 hours under an argon atmosphere, followed by reheating to 650 ℃ for 8 hours in an inert gas environment, with a heating rate of 5 ℃/min.

Cell assembly and electrochemical measurements

The cathode material was mixed with conductive carbon black and PVDF binder in an NMP solvent at a mass ratio of 8:1:1 to form a uniform slurry. The slurry was then cast on an Al foil and vacuum-dried at 80 ºC for 8 h. The above electrode film was cut into round discs with a diameter of 12 mm. The CR2025 coin cells were then assembled in an Ar-filled glovebox using Celgard 2400 membrane as the separator, Li metal foil as the counter electrode, and 1 mol L^{-1} LiPF6 (EC: DEC: DMC = 1:1:1 as solvent, volume ratio) as the electrolyte. Subsequently, galvanostatic charge/discharge tests were conducted on a LAND CT2001A battery tester in the voltage window of 2.5-4.2 V versus Li/Li^+. CV with a sweep rate of 0.1 mV S^{-1} and a voltage range of 2.5-4.2 V and EIS measurements in the frequency range of 0.01 Hz-100 kHz were carried out on a Solartron Analytical instrument.

Instrumentation

ICP-OES tests were conducted on a SHIMADZU ICPE-9000 spectrometer. X-ray diffraction (XRD) analysis was conducted to identify the composition of the synthesized materials. Transmission electron microscopy (TEM), scanning electron microscopy (SEM), and high-angle annular dark-field scanning transmission electron microscopy (HAADF-STEM) were employed to analyze the morphology and structure of the recovered LFP materials. X-ray photoelectron spectroscopy (XPS) measurements were carried out on a Thermo Fischer ESCALAB Xi+ instrument to determine the composition and valence states of the recovered LFP. An inductively coupled plasma optical emission spectrometer (ICP-OES) was used to analyze the elemental content of $Li_{0.95}Na_{0.05}FePO_4$.

Environmental and economic analysis

The EverBatt model developed by Argonne National Laboratory and the prospective cradle-to-

gate life cycle analysis (LCA) were employed to analyze different recycling routes on a per-unit-mass basis for spent $LiFePO_4$ batteries. The energy consumption and economic analysis for this work were calculated based on the process parameters obtained in our laboratory. Moreover, hydrometallurgical recycling route, traditional direct recycling route, and this work were calculated based on a combination of the typical process from EverBatt model and reported in literature [1-3]. The details of the calculations and parameters are shown in Table S2-S10.

The total energy consumption for each recycling route was calculated as formula (1):

$$E_{\text{total}} = \sum_i m_i \times e_{u,i} + \sum_i n_i \times e_{v,i} + j \quad (1)$$

where m_i is the mass of input material i, $e_{u,i}$ is the unit embodied energy of material i (from EverBatt database), n_i is the consumption of input energy i during the process, and $e_{v,i}$ is the unit energy intensity of energy i, j is other input costs, including battery fee, process waste management, labour and fixed assets (from EverBatt database).

The total recycling cost encompasses the costs of materials, energy, and other miscellaneous inputs. It is calculated as formula (2):

$$\text{Recycling cost} = \sum_i m_i \times up_i + \sum_i n_i \times vp_i + k \quad (2)$$

Here, m_i is the mass of input material i, up_i is the unit price of input material i, and vp_i is the unit price of the process energy. The parameter k accounts for other fixed and variable costs, including battery acquisition, waste disposal, labor, and overhead expenses, all of which were derived from the EverBatt model.

The total revenue generated from the recycled materials was calculated based on the market value of the recovered products. It is calculated as formula (3):

$$\text{Revenue} = \sum_i m_i \times rp_i \quad (3)$$

where m_i is the mass of input material i, and rp_i represents its unit market price.

Profit is the difference between revenue and recovered costs (formula (4)):

$$Profit = Revenue - Recycling\ cost \quad (4)$$

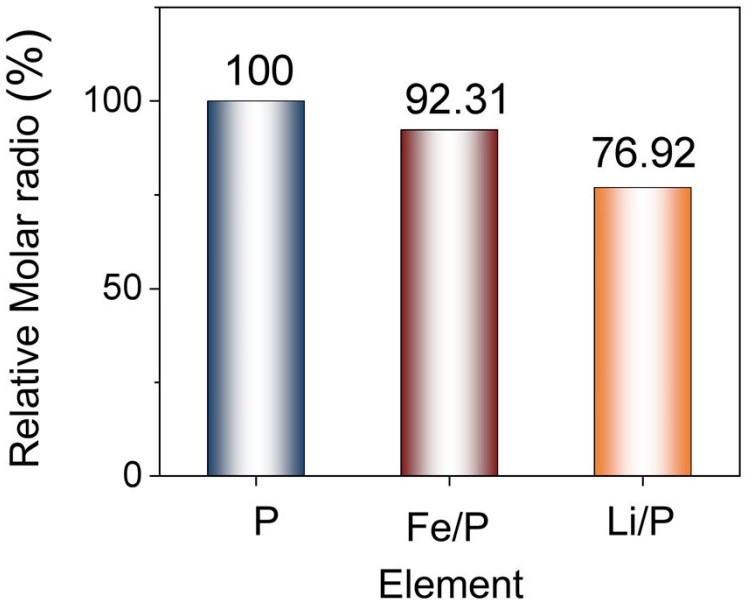

Supplementary Fig. 1 Molar ratio of each element in spent $LiFePO_4$.

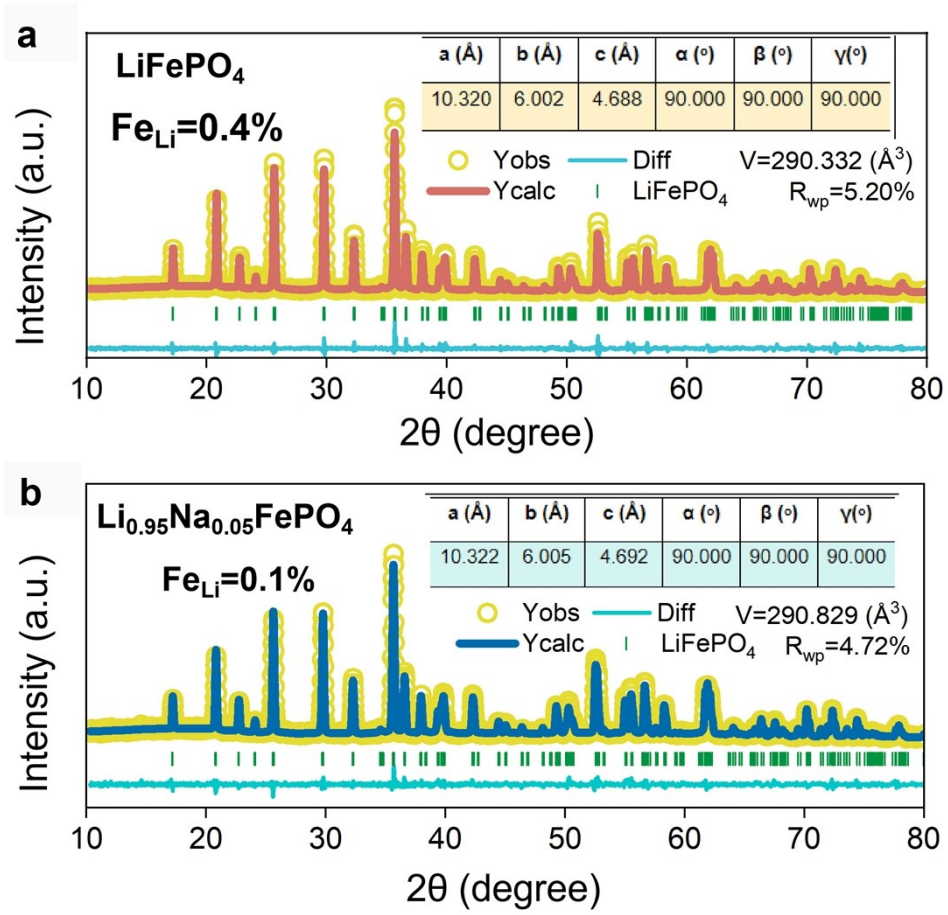

Supplementary Fig. 2 (a) Rietveld-refined XRD patterns of $LiFePO_4$ (Fe_{Li} = 0.4%). (b) Rietveld-refined XRD patterns of $Li_{0.95}Na_{0.05}FePO_4$ (Fe_{Li} = 0.1%).

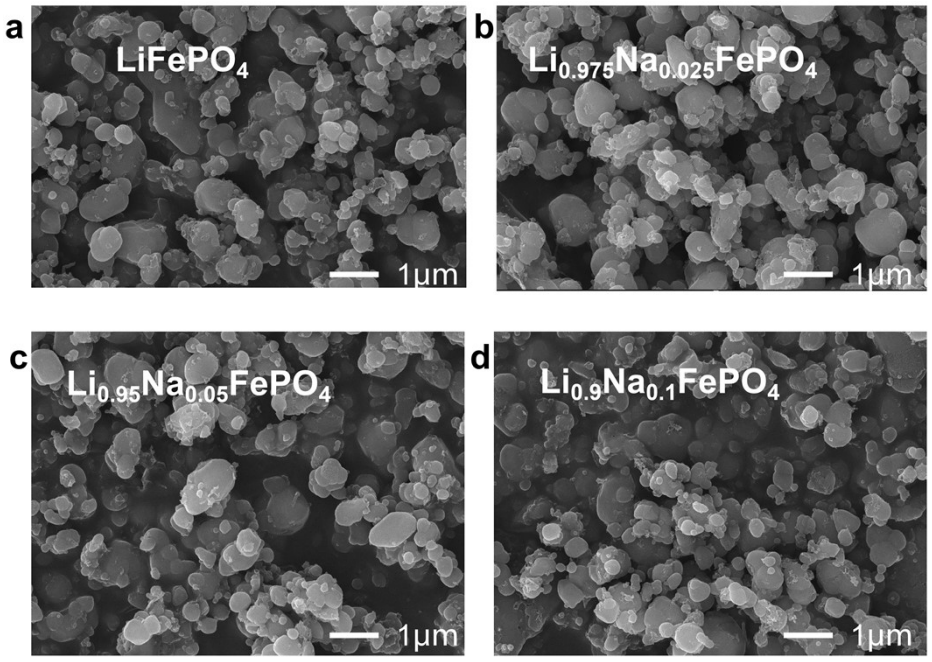

Supplementary Fig. 3 (a) SEM image of $LiFePO_4$. (b) SEM image of $Li_{0.975}Na_{0.025}FePO_4$. (c) SEM image of $Li_{0.95}Na_{0.05}FePO_4$. (d) SEM image of $Li_{0.9}Na_{0.1}FePO_4$.

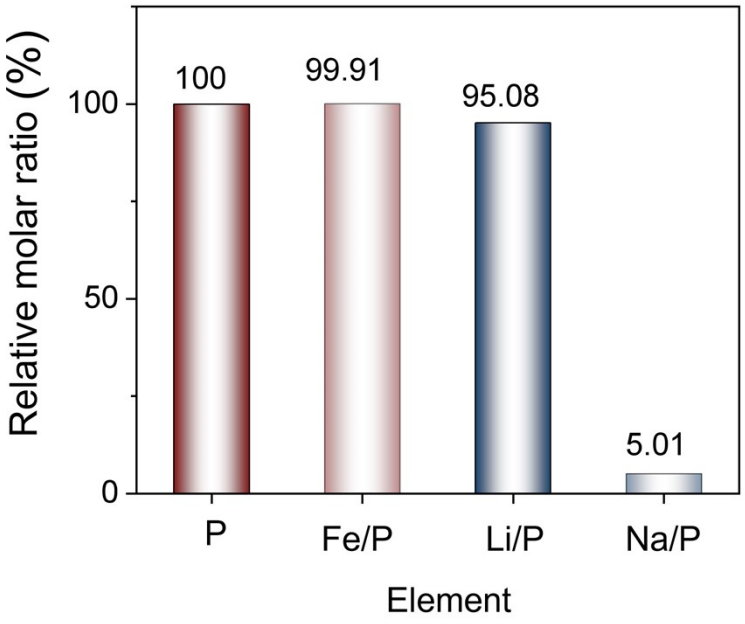

Supplementary Fig. 4 Molar ratio of each element of $Li_{0.95}Na_{0.05}FePO_4$.

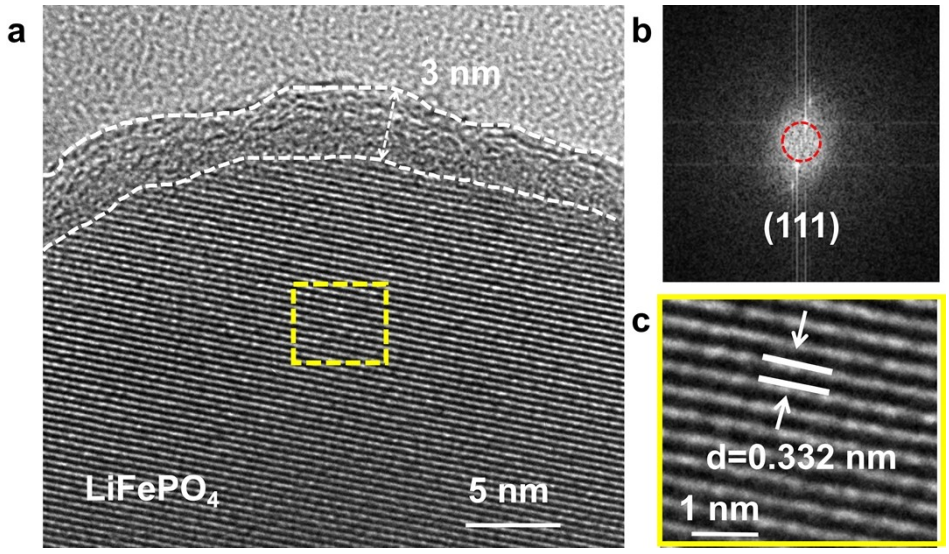

Supplementary Fig. 5 (a) The high-resolution TEM image of $LiFePO_4$. (b) the Fast-Fourier-Transform (FFT) pattern of $LiFePO_4$. (c) lattice spacing analysis of $LiFePO_4$.

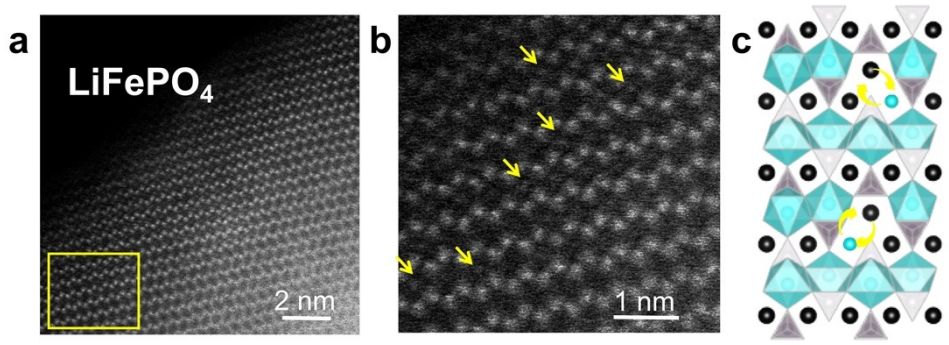

Supplementary Fig. 6 (a) AC STEM-HAADF-EDS mapping images of $LiFePO_4$. (b) HRTEM images of $LiFePO_4$. (c) Structural representation of Li-Fe anti-sites.

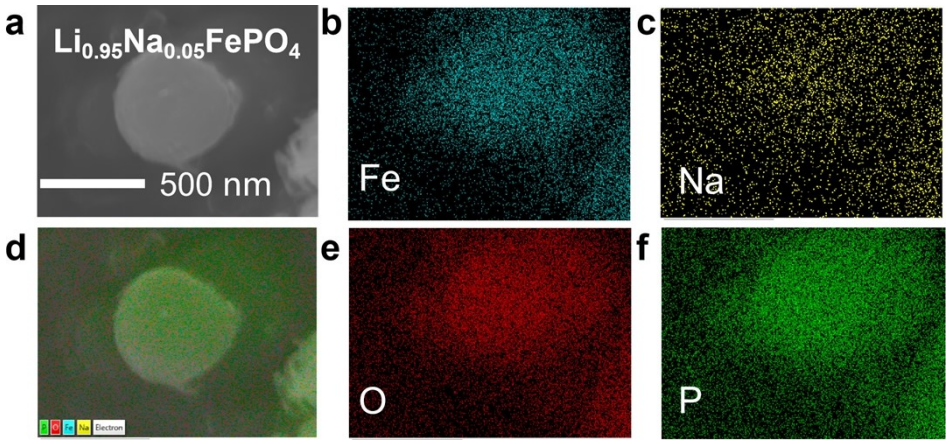

Supplementary Fig. 7 (a) The scanning transmission electron microscopy (STEM) image of $Li_{0.95}Na_{0.05}FePO_4$**.** (b-f) The corresponding energy-dispersive X-ray spectroscopy (EDS) elemental mapping images of Fe, Na, O, and P in the $Li_{0.95}Na_{0.05}FePO_4$ particle.

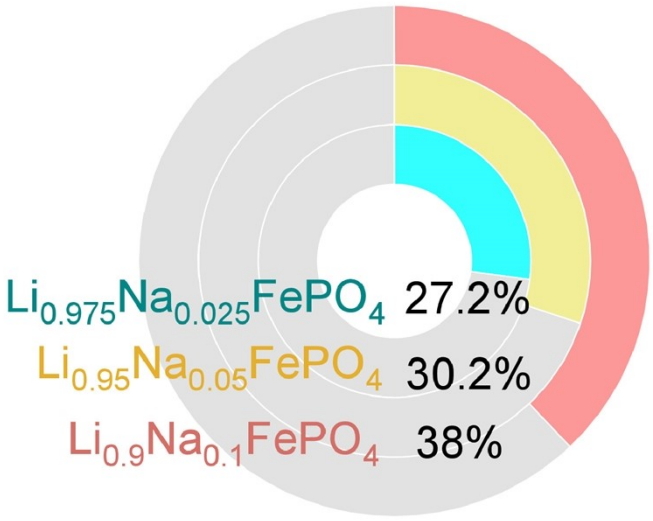

Supplementary Fig. 8 The relative ratio of Fe^{2+} to Fe^{3+} content**.**

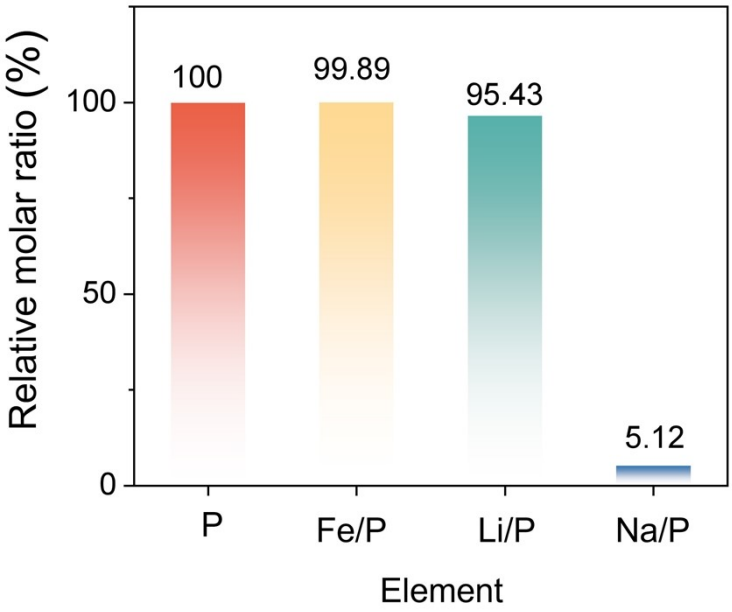

Supplementary Fig. 9 Molar ratio of each element of $Li_{0.95}Na_{0.05}FePO_4$ after charging.

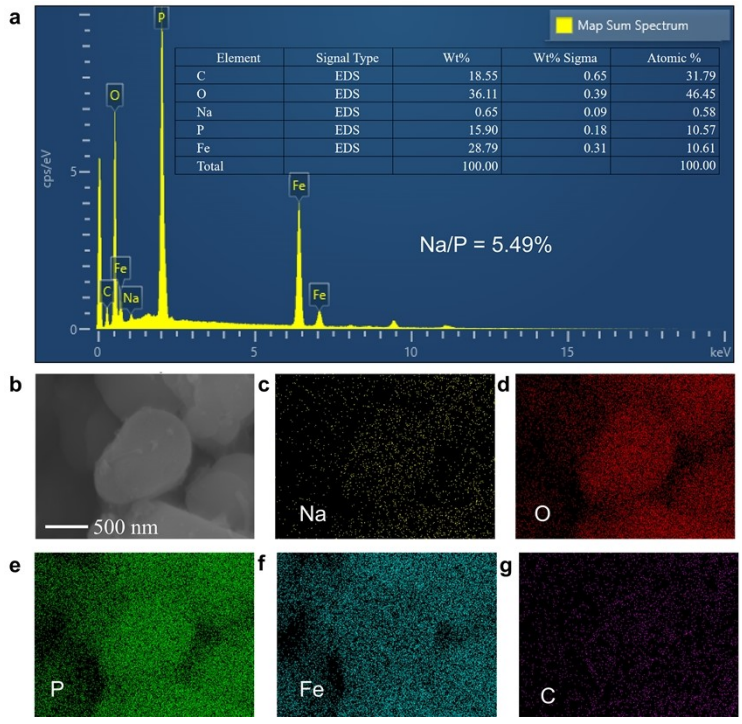

Supplementary Fig. 10 (a) EDS survey spectrum of $Li_{0.95}Na_{0.05}FePO_4$ particle after charging. (b-g) The corresponding EDS elemental mapping images of Fe, Na, O, C, and P in the $Li_{0.95}Na_{0.05}FePO_4$ particle after charging.

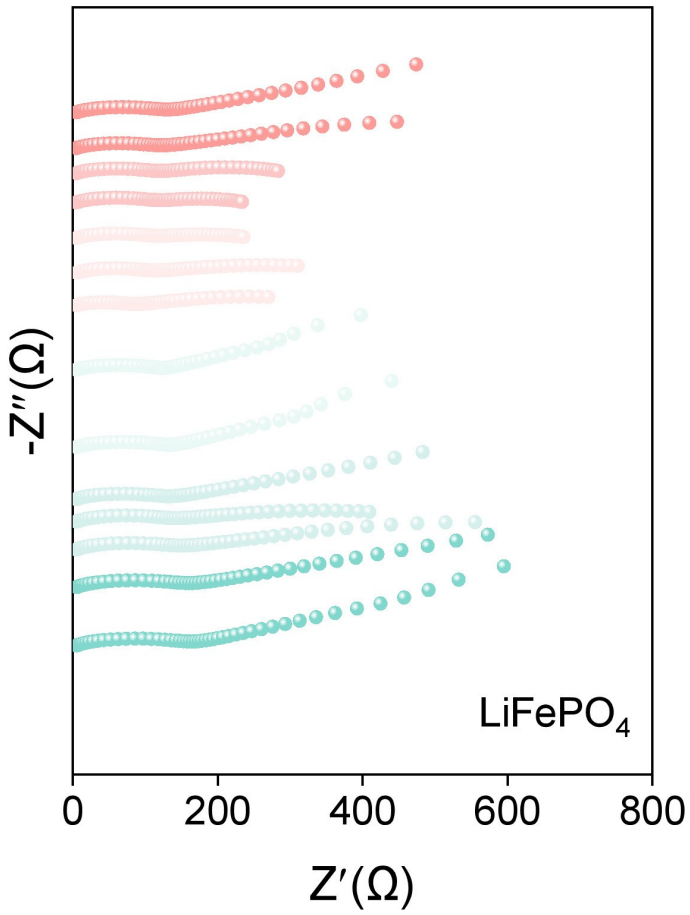

Supplementary Fig. 11 The in-situ EIS of cycled $LiFePO_4$ during charge/discharge.

Supplementary Eq. 1

$$2d \sin\theta = n\lambda$$

In this equation, d is the distance between adjacent parallel crystal planes, θ is the Bragg angle (half the angle between incident and diffracted X-rays), n is the positive integer diffraction order, and λ is the fixed wavelength of the incident X-ray (determined by the testing equipment)[4].

Supplementary Eq. 2

$$Ip = 2.69 \times 10^5 \times n^{2/3} AD^{1/2} v^{1/2} C_{Li+}$$

In this equation, *Ip* is the peak current, n is the number of electrons transferred during the reactions, A is the surface area of active electrodes (1.13 cm^2), v indicates the scan rate, and C_{Li+} is the Li-ions concentration of the LFP lattice[5].

Supplementary Table 1. The comparison of regenerated LFP samples in previous work and this work.

Samples	Capacity ($mAh\ g^{-1}$, C)	Capacity retention	Ref.
regenerated LFP	147.9 at 1 C	86% after 500 cycles at 5 C	6
regenerated LFP	144 at 1 C	96% after 500 cycles at 5 C.	7
regenerated LFP	152.5 at 0.1 C	98.7% after 200 cycles at 1 C.	8
regenerated LFP	142.7 at 1 C	no degradation after 200 cycles at 1 C.	9
regenerated LFP	150.5 at 0.5 C	94.9% after 500 cycles at 0.5 C.	10
regenerated LFP	155.6 at 0.1 C	93% after 300 cycles at 1 C.	11
regenerated LFP	142.9 at 1 C	Nearly 100% after 200 cycles at 1 C.	12
regenerated LFP	164.2 at 0.1 C	93.1% after 800 cycles at 5 C.	13
regenerated LFP	150.0 at 0.2 C	82% after 300 cycles at 1 C.	14
regenerated LFP	124.3 at 2.0 C	92.1% after 400 cycles at 2 C.	15
$Li_{0.95}Na_{0.05}FePO_4$	116.2 at 5.0 C	99 % after 400 cycles at 5 C.	This work

Supplementary Table 2. The process parameters for hydro process.

Process		Item	Dosage	Unit	Notes
Crushing and screening	Input	spent LIBs	1.00	kg	1 MJ electricity produces 0.13 kg GHG and 0.67 L water. 1 kg diesel produces 45.6 MJ energy. The data is estimated based on Everbatt 2020. ~5 wt% NaCl solution is adopted for safe discharging.[4]
		Energy	2.87	MJ	
	Output	LFP powder	0.35	kg	
		Cu/Al/steel	0.4	kg	
		graphite	0.17	kg	
		GHG	0.255	kg	
Acid leaching	Input	LFP powder	0.35	kg	Pulp density 10 g/L, 60°C at 200 rpm for 2 h, 1 mol/L H_2SO_4, 6% H_2O_2. Leachate contained 3.54 g/L Fe and 0.44 g/L of Li.[2]
		H_2SO_4	0.52	kg	
		H_2O_2	0.76	L	
		Energy	12.35	MJ	
	Output	Leaching slag	0.41	kg	
		Leachate	1.48	kg	
		GHG	0.406	kg	
Slag purification	Input	Leaching slag	0.41	kg	

	Output	Energy	0.68	MJ	
		$FePO_4$	0.33	kg	
		GHG	0.193	kg	
Leachate purification	Input	Leachate	1.48	L	PH adjusted to 9.0-10.0 for Li_2CO_3 precipitation. The solution degree of Na_2CO_3 is 40 g/100g (30°C).
		Na_2CO_3	0.15	kg	
		NaOH	0.68	kg	
	Output	Energy	0.71	MJ	
		Li_2CO_3	0.065	kg	
		GHG	0.284	kg	
Fabrication	Input	$FePO_4$	0.33	kg	Recycled $FePO_4$ and Li_2CO_3 were mixed and calcined at 700 °C for 6 h under inert atmosphere to regenerate battery-grade LFP cathode material.
		Li_2CO_3	0.065	kg	
		Energy	4.175	MJ	
	Output	R-LFP	0.28	kg	
		GHG	0.612	kg	

Supplementary Table 3. Cost analysis of hydro process.

Item		Dosage	Unit	Unit price	Cost ($)	Data source
Energy		20.941	MJ	0.0186 $/kWh	0.108	EverBatt
	H_2SO_4	0.52	kg	0.15 $/kg	0.076	SMM
	H_2O_2	0.76	kg	0.39 $/kg	0.298	SMM
	NaOH	0.68	kg	0.31 $/kg	0.213	SMM
	Na_2CO_3	0.15	kg	2.16 $/kg	0.324	SMM
Battery fee		1	kg	3.86	3.86	Mysteel
Process		/	/	/	0.6	EverBatt 2020
Waste management		/	/	/	0.45	EverBatt 2020
Labor		/	/	/	0.52	EverBatt 2020
Fixed assets		/	/	/	0.561	EverBatt 2020
		Cost ($/kg)			7.01	

Supplementary Table 4. The process parameters for direct process.

Process		Item	Dosage	Unit	Notes
Dismantling	Input	spent LIBs	1.00	kg	1 MJ electricity produces 0.13 kg GHG and 0.67 L water. 1 kg diesel produces 45.6 MJ energy. The data is estimated based on Everbatt 2020. ~5 wt% NaCl solution is adopted for safe discharging.
		Energy	2.87	MJ	
		cathode scrap	0.44	kg	
		separator/steel	0.28	kg	
		Anode scrap	0.26	kg	
	Output	GHG	0.038	kg	

Soaking	Input	cathode sheet	0.44	kg	To separate the active materials from Al foils to decompose the binder, large of deionized water is needed.
		Energy	0.156	MJ	
		Water	0.35	kg	
	Output	D-LFP	0.35	kg	
		Al foil	0.07	kg	
		GHG	0.217	kg	
Relithiation/Annealing	Input	D-LFP	0.35	kg	was preheated at 350 °C for 4 hours under an argon atmosphere, followed by reheating to 650 ℃ for 8 hours in an inert gas environment, with a heating rate of 5 ℃/min.
		Li_2CO_3	0.02	kg	
		Sucrose	0.06	kg	
		Energy	1.422	MJ	
	Output	R-LFP	0.31	kg	
		GHG	0.695	kg	

Supplementary Table 5. Cost analysis of direct approach.

Item		Dosage	Unit	Unit price	Cost ($)	Data source
Energy		4.448	MJ	0.0186 $/kWh	0.023	EverBatt 2020
	Sucrose	0.06	kg	0.43 $/kg	0.026	SMM
	Li_2CO_3	0.02	kg	13.8 $/kg	0.276	SMM
Battery fee		1	kg	3.86 $/kg	3.86	Mysteel
Process		/	/	/	0.42	EverBatt 2020
Waste management		/	/	/	0.6	EverBatt 2020
Labor		/	/	/	0.38	EverBatt 2020
Fixed assets		/	/	/	0.215	EverBatt 2020
Cost ($/kg)					5.8	

Notes: SMM (https://www.smm.cn/); Mysteel (https://m.mysteel.com/).

Supplementary Table 6. The process parameters for this work.

Process		Item	Dosage	Unit	Notes
Dismantling	Input	spent LIBs	1.00	kg	1 MJ electricity produces 0.13 kg GHG and 0.67 L water. 1 kg diesel produces 45.6 MJ energy. The data is estimated based on Everbatt 2020. ~5 wt% NaCl solution is adopted for safe discharging.
		Energy	2.87	MJ	
		cathode scrap	0.44	kg	
		separator/steel	0.28	kg	
		Anode scrap	0.26	kg	
	Output	GHG	0.038	kg	
Soaking	Input	cathode sheet	0.44	kg	To separate the active materials from Al foils to decompose the binder, large of deionized water is needed.
		Energy	0.156	MJ	
		Water	0.35	kg	
	Output	D-LFP	0.35	kg	
		Al foil	0.07	kg	
		GHG	0.217	kg	
Relithiation/Annealing	Input	D-LFP	0.35	kg	was preheated at 350 °C for 4 hours under an argon atmosphere, followed by reheating to 650 °C for 8 hours in an inert gas environment, with a heating rate of 5 °C/min.
		Li_2CO_3	0.015	kg	
		Na_2CO_3	0.007	kg	
		Sucrose	0.06	kg	
		Energy	0.802	MJ	
	Output	R-LFP	0.31	kg	
		GHG	0.395	kg	

Supplementary Table 7. Cost analysis of direct approach.

Item		Dosage	Unit	Unit price	Cost ($)	Data source
Energy		3.828	MJ	0.0186 $/kWh	0.020	EverBatt 2020
	Sucrose	0.06	kg	0.43 $/kg	0.026	SMM
	Li_2CO_3	0.015	kg	13.8 $/kg	0.212	SMM
	Na_2CO_3	0.007	kg	2.16 $/kg	0.015	SMM
Battery fee		1	kg	3.86 $/kg	3.86	Mysteel
Process		/	/	/	0.42	EverBatt 2020
Waste management		/	/	/	0.258	EverBatt 2020
Labor		/	/	/	0.144	EverBatt 2020
Fixed assets		/	/	/	0.215	EverBatt 2020
Cost ($/kg)					5.17	

Notes: SMM (https://www.smm.cn/); Mysteel (https://m.mysteel.com/).

Spplementary Table 8. Revenue and profit of different recycling approaches ($ kg^{-1}, cell).

		Hydro	Direct	This work
Revenue	Al	0.22	0.22	0.22
	LFP	3.99	11.88	14.69
Cost		7.01	5.8	5.17
Profit		-2.8	6.3	9.74

Supplementary Table 9. LCA of different recycling approaches.

	Hydro	Direct	This work
Total energy (MJ kg^{-1}, cell)	20.941	4.448	3.828
Fossil fuels	14.265	3.752	3.186
Coal	4.425	2.316	2.154
Natural gas	4.518	0.362	0.315
Diesel (kg kg^{-1})	0.115	0.081	0.712
VOC	0.338	0.235	0.208
CO	1.426	0.892	0.816
NOx	3.582	1.914	1.825
PM10	0.235	0.241	0.236
PM2.5	0.188	0.155	0.142
SOx	0.765	1.312	1.245
BC	0.101	0.030	0.027
OC	0.037	0.028	0.026
CH_4	2.015	2.531	2.486
N_2O	0.026	0.033	0.031
CO_2	1256	1618	1546
CO_2 (w/C in VOC & CO) (scaled)	1328	1635	1552
GHG (kg kg^{-1} cell)	1.75	0.95	0.65
Revenue ($ kg^{-1}, cell)	4.21	12.1	14.91
Cost ($ kg^{-1}, cell)	7.01	5.8	5.17
Profit ($ kg^{-1}, cell)	-2.8	6.3	9.74

Supplementary Table 10. Energy consumption of different recycling methods (MJ kg^{-1}, cell).

Methods	**Material input**	**Energy input**
Hydro-	14.512	6.429
Direct	4.036	0.412

Methods	Material input	Energy input
This work	3.472	0.356

Reference

1. Lv, X. W.; Lin, J.; Zhang, X. D.; Huang, Q. R.; Sun, X.; Fan, E. S.; Chen, R. J.; Wu, F. and Li, L., *Adv. Energy Mater.*, 2024, **14**, 2402560.
2. Xu, P.; Dai, Q.; Gao, H.; Liu, H.; Zhang, M.; Li, M.; Chen, Y.; An, K.; Meng, Y. S.; Liu, P.; Lu, J.; Chen, Z., *Joule*, 2020, **4**, 2609-2626.
3. Wang, X. J.; Zheng, S. L.; Zhang, Y.; Zhang, Y.; Qiao, S.; Long, Z. Q.; Zhao, B. and Li, Z. F., *Waste Manage.*, 2022, **153**, 31-40.
4. J. Li, S. Li and Q. Li, Mater. *Res. Innov.*, 2015, **19**, 4.
5. H. Xue, Y. Wu, Z. Wang, Y. Shen, Q. Sun, G. Liu, D. Yin, L. Wang, Q. Li and J. Ming, *ACS Appl. Mater. Interfaces*, 2021, **13**, 40471-40480.
6. D. Tang, G. J. Ji, J. X. Wang, Z. Liang, W. Chen, H. C. Ji, J. Ma, S. Liu, Z. F. Zhuang and G. M. Zhou, *Adv. Mater.*, 2024, **36**, 2309722.
7. J. Tang, H. T. Qu, C. B. Sun, X. Xiao, H. C. Ji, J. X. Wang, J. F. Li, G. J. Ji, X. Zhang, H. M. Cheng and G. M. Zhou, *Adv. Mater.*, 2025, **37**, 2420238.
8. L. Q. Zhang, H. P. Gao, Y. W. Zhu, I. Tran, W. Tang, J. Lin, A. U. Mu, J. L. Wu, W. Li, D. Nordlund and D. Wang, *Adv. Energy Mater.*, 2025, **15**, 2406084.
9. L. Yang, B. C. Zhang, S. Chen, Q. Pan, W. Y. Li, C. L. Gan, W. T. Deng, G. Q. Zou, H. S. Hou and J. Liu, *Chem. Commun.*, 2024, **60**, 9384-9387.
10. S. P. Hao, Y. L. Lv, Y. Zhang, S. W. Liu, Z. L. Tan, W. Liu, Y. G. Xia, W. Yin, Y. Q. Liao, H. J. Ji and M. Liu, *Energy Environ. Sci.*, 2025, **18**, 3750-3760.
11. Y. X. Lin, T. S. Wang, C. C. Gao, X. X. Zhang, W. Yu, M. Wang, C. Yang and J. H. Zhang, *Adv. Sci.*, 2025, **12**, 2504683.
12. Y. Y. Li, Q. F. Liu, W. Q. Yu, C. C. Li, Z. T. Fei, Q. Meng and P. Dong, *Sep. Purif. Technol.*, 2025, **370**, 133059.
13. S. R. Nie, Y. H. Xia, Y. Z. Xiao, W. H. Lin, G. Y. Yang, W. L. Peng, S. K. Peng, F. B. Meng, R. Z. Hu and B. Yuan, *ACS Appl. Mater. Interfaces*, 2025, **17**, 21257-21268.
14. T. S. Wang, C. C. Gao, Z. Q. Zheng, W. Yu, M. Wang, C. Yang and J. H. Zhang, *Adv. Funct. Mater.*, 2025, **35**, 2502930.
15. Y. Y. Liu, J. Bai, R. Y. Shi, P. Y. Wang, K. Xiao, S. Y. Wang, S. Y. Qiu, X. L. Wang, X. B. Zhu, K. S. Yang and M. Liu, *Adv. Mater.*, 2025, e11246.
16. J. Lin, E. Fan, X. Zhang, Z. Li, Y. Dai, R. Chen, F. Wu and L. Li, *Adv. Energy Mater.*, 2022, **12** 2201174.